

R. J. Bucci,<sup>1</sup> P. C. Paris,<sup>1</sup> J. D. Landes,<sup>2</sup> and J. R. Rice<sup>3</sup>

## *J* Integral Estimation Procedures

REFERENCE: Bucci, R.J., Paris, P.C., Landes, J.D., and Rice, J.R., "J Integral Estimation Procedures," *Fracture Toughness, Proceedings of the 1971 National Symposium on Fracture Mechanics, Part II, ASTM STP 514*, American Society for Testing and Materials, 1972, pp. 40-69.

ABSTRACT: By making use of plastically adjusted linear elastic fracture mechanics analysis and plastic limit load solutions, a method is developed for reasonable approximation of Rice's path independent *J* integral which is applicable for test specimens or other configurations which exhibit considerable plasticity prior to fracture. Employing this, *J* is expressed as a function of load point displacement. Estimations of the *J* versus displacement relationships developed compared quite well to those previously established experimentally at Westinghouse Research Laboratories for Ni-Cr-Mo-V and A533B steels. For these comparisons, the test specimen configurations considered were three point bend, center notch, and compact tension test specimen configurations, all of which exhibit significantly different plastic limit load slip line flow fields. Thus, the method developed for approximating *J* is thought to be widely applicable.

KEY WORDS: fracture (materials), fracture strength, toughness, loads (forces), tensile properties, plastic analysis, stressing, cracking (fracturing), elastic limit, plastic limit, tension tests, fracture tests, alloy steels

Recent experiments by Begley and Landes [1] have demonstrated the potential of Rice's path independent integral, *J* [2], as an effective criterion for the initiation of crack extension. The critical *J* fracture criterion was found to be applicable for situations which sustain either small or large scale plasticity prior to fracture. Therefore, if such results continue to prevail, a significant extension of fracture toughness concepts into the plastic range has been discovered.

The *J* integral is defined for two dimensional problems and is given by [2]

$$J = \int_R W dy - T \cdot \frac{\partial u}{\partial x} ds \quad (1)$$

<sup>1</sup> Del Research Corporation, Hellertown, Pa. 18055.

<sup>2</sup> Research and Development Center, Westinghouse Electric Corporation, Pittsburgh, Pa. 15235.

<sup>3</sup> Brown University, Providence, R.I. 02912.

where  $W$  is the strain energy density as defined by

$$W = W(\epsilon_{ij}) = \int_0^{\epsilon_{ij}} \sigma_{pq} d\epsilon_{pq} \quad (2)$$

and as shown in Fig. 1,  $R$  is any contour surrounding the crack tip,  $\mathbf{T}$  is a traction vector defined by outward normal  $m$  along  $R$ ,  $T_i = \sigma_{ij}m_j$ ,  $\mathbf{u}$  is the displacement vector, and  $s$  is arc length along  $R$ . For any elastic or elastic-plastic material treated by deformation theory of plasticity, Rice [2] has proven path independence of the  $J$  integral. Other recent studies [3, 4] using incremental theory for finite element analysis also demonstrate an approximate path independence within the plastic region, although it is not clear that this prevails for contours immediately adjacent to the crack tip [5].

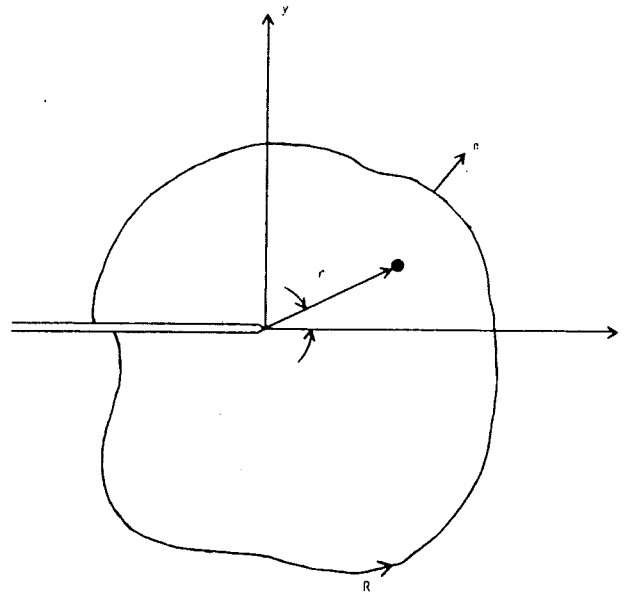


FIG. 1—Crack tip coordinate orientation and arbitrary line integral contour.

An alternate and equivalent interpretation [6] of  $J$  for elastic (linear or non-linear) materials is that of a potential energy difference for identically loaded configurations having neighboring crack sizes  $a$  and  $a + da$ . In particular

$$J = - \frac{\partial (U/B)}{\partial a} \quad (3)$$

where  $U/B$  is the potential energy normalized per unit thickness  $B$ . This is defined by

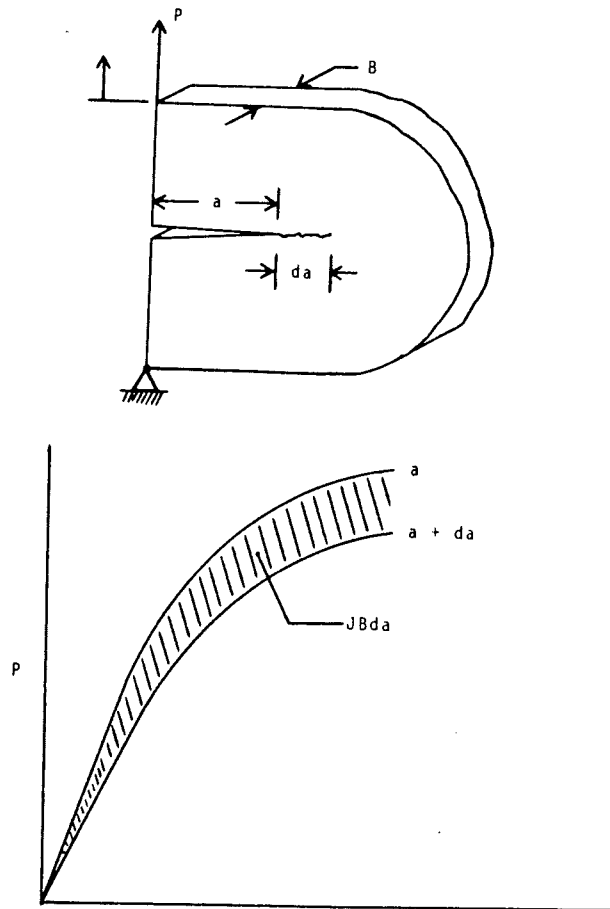
$$U/B = \iint_A W dx dy - \int_{c_t} \mathbf{T} \cdot \mathbf{u} ds \quad (4)$$

where  $W$  is the strain energy density and  $c_t$  that portion of boundary contour on which tractions  $\mathbf{T}$  are prescribed. For elastic-plastic materials, we shall take Eq 3 as defining  $J$ , where it is to be understood that the *pseudo-potential energy*  $U/B$  corresponding to any given crack length is defined by Eq 4 with  $W$  then being the work of stress deformation as experienced during monotonic increase of the boundary loads on a body which has that same crack length in an unloaded reference state. This precision of definition is necessary in view of the dependence of plastic response on prior deformation history. Within the context of deformation plasticity theory, the above definition of  $J$  is equivalent to that as given by the line integral Eq 1 although a similar equivalence cannot be proven for actual incremental plastic materials. In analogy with the linear elastic fracture mechanics interpretation of the energy release rate [7, 8], the area between two monotonic load deflection curves for neighboring crack sizes  $a$  and  $a + \Delta a$  is, from the adopted definition of  $J$ ,  $BJ\Delta a$  to first order. This interpretation is illustrated in Fig. 2; moreover, it allows rather simple calculations of  $J$  as will be developed herein.

Noting the above interpretations, Begley and Landes [1] previously developed a procedure which permits  $J$  evaluation from a family of load-displacement records experimentally determined from test specimens of varying initial crack length. Their suggested procedure for this calculation is outlined in Appendix 1 and amplified in Ref 1.

Equations 1 and 3 may be physically regarded as characterizing the Applied  $J$  and as providing methods of evaluating the  $J$  imposed by external sources. On the other hand the  $J$ , so imposed, causes processes to occur in the vicinity of the crack tip in such a way that  $J$  may be regarded as a measure of the resulting crack tip field of deformation. Thus, the  $J$  integral characterizes the near tip stress-strain environment of cracked elastic-plastic bodies, which offers the distinct advantage that it is possible to characterize the local crack tip phenomena by a single field parameter which does not focus attention directly to specific crack tip features. This is again analogous to the linear elastic fracture mechanics interpretation that the extent of the near tip process may be evaluated in terms of the imposed crack tip stress field intensity,  $K$ , or its equivalent elastic strain energy release rate,  $G$ . It is noted that in fact  $J$  approaches  $G$  in the limit of the purely elastic case. It remains, however, an open question as to the suitability of a one-parameter characterization in the large scale yielding range.

Hopefully, the  $J$  integral representation of fracture can be successful so long as the stress strain environment within some "fracture process zone" is

FIG. 2—Interpretation of  $J$  integral.

dominated by conditions local to the crack tip leading edge and is also insensitive to length factors such as crack size, net ligament, and thickness [9, 10]. Moreover, deformation theory of plasticity is meaningless when unloading occurs and this implies that substantial subcritical crack extension (beyond that associated with plastic blunting of the tip) is not permitted. Therefore, the  $J$  fracture criterion must presently be restricted to crack initiation rather than propagation, as indicated by Begley and Landes [1]. However, these restrictions might not turn out to be any more restrictive than those caused by analogous plasticity effects in linear elastic fracture mechanics, and local unloading would then be admissible within some size of region which might be analogously described as proportional to  $J/\sigma_{ys}$ , where  $\sigma_{ys}$  is the tensile yield stress. In spite of these apparent "size" limitations [9, 10], the determination of which must be

left largely to experiment, Begley and Landes have demonstrated with success [1] that relatively small specimens which exhibit fracture at full limit load conditions satisfy these dimensional requirements and provide valid interpretation of the  $J$  criterion. For both a low and intermediate strength steel, Begley and Landes [1] were able to determine experimentally a critical plane strain  $J$  value ( $J_{Ic}$ , which satisfied "degree of plastic restraint" requirements) at which elastic-plastic and fully plastic fracture occurred for a variety of crack lengths and specimen types. Their critical  $J_{Ic}$  determination was consistent with the linear elastic fracture mechanics interpretation of  $G_{Ic}$ . That is, their critical plane strain  $J_{Ic}$  obtained from smaller fully plastic specimens agreed favorably with critical  $G_{Ic}$  obtained from fracture of large specimen configurations which satisfied ASTM plane strain criterion [11].<sup>4</sup>

### Objectives

Encouraged by the experimental success of Begley and Landes and their development of a fracture criterion based on the  $J$  integral, an attempt is made here to provide simple but effective approximate methods of calculating the "applied"  $J$  utilizing a minimum amount of concomitant supporting experimental effort.

The Begley and Landes procedure [1] (outlined in Appendix 1) used for the establishment of a relationship between  $J$  and the load point displacement,  $\delta$ , required both procurement and analysis of a large number of experimental load-displacement records, which is both time consuming and costly. It would be a great advantage and is an objective herein to be able to estimate the  $J$  versus  $\delta$  relationship for a given test specimen configuration and from this, supplemented by *one* experimental load-displacement record (which determines a displacement at fracture), establish a critical value of  $J$ .

For practical structural applications where more complex flaw and loading geometries are apparent, a purely experimental evaluation of the  $J$  versus  $\delta$  relationship may not always be conveniently possible. If, for these practical component-flaw geometries, one could make meaningful  $J$  versus  $\delta$  approximations, derived using no more than linear elastic fracture mechanics and plastic limit analysis, then along with critical  $J$  (or  $G$ ) values established from simpler test configurations, one might effect reasonable predictions for loads and load point displacements at fracture, and hence, for practical applications, establish critical flaw sizes or design stress levels or both.

Towards the achievement of the above goals, the primary purpose of this work is to provide simple but effective methods for approximating the  $J$  versus  $\delta$  relationship based on no more than linear elastic fracture mechanics and plastic

<sup>4</sup>For a valid fracture criterion,  $J_{Ic}$  should equal  $G_{Ic}$ . Since for small scale yielding  $J$  is identical to  $G$ , this implies that  $J_{Ic}$  may be related to plane strain fracture toughness,  $K_{Ic}$ , as  $J_{Ic} = (1-\nu^2) K_{Ic}^2 / E$ .

limit analysis. The effectiveness of the approximating techniques will be evaluated for three common test specimen configurations, the three point bend bar, the center notch, and compact tension specimen, all of which exhibit grossly different limit load slip line fields [12]. In order to judge the analytically developed expressions for the  $J$  versus  $\delta$  relationship, they will be compared to those experimentally established by Begley and Landes [1] for Ni-Cr-Mo-V and A533B steels.

### Some Useful Observations

Following the  $J$  interpretation outlined earlier, and also discussed in Appendix 1, that  $J$ , as given by Eq 3, may simply be evaluated from the area between load-deflection curves of slightly different crack lengths, it becomes relevant to examine one's ability to generate reasonable estimates of load-displacement behavior for cracked configurations and especially their variation with crack size. The limiting cases of load-displacement character are those exhibited by either purely elastic or rigid plastic behavior, Fig. 3a. For the pure elastic case,  $J$  is identical to  $G$ , the energy release rate [1], and may be expressed as [13]

$$J = G = \frac{P^2}{2} \frac{\partial \lambda}{B \partial a} \quad (5)$$

where  $P$  is the applied load,  $\partial a$  represents an increment of crack extension,  $B$  is the material thickness, and where load and displacement are related by

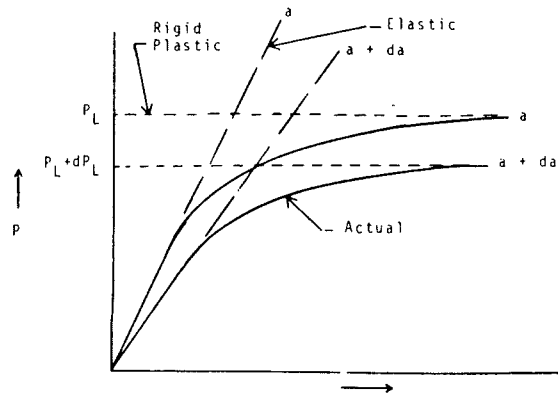
$$\delta = \lambda P \quad (6)$$

$\lambda$  is an inverse spring constant, or compliance which is a function of flaw size, specimen geometry, and elastic material constants, namely,  $E$ , Young's modulus, and sometimes  $\nu$ , Poisson's ratio. Since Eq 6  $J$  is proportional to  $\delta^2$ ,  $J$  as a function of  $\delta$ , for pure elastic behavior, assumes the form of a parabola for a given constant crack size, Fig. 3b.

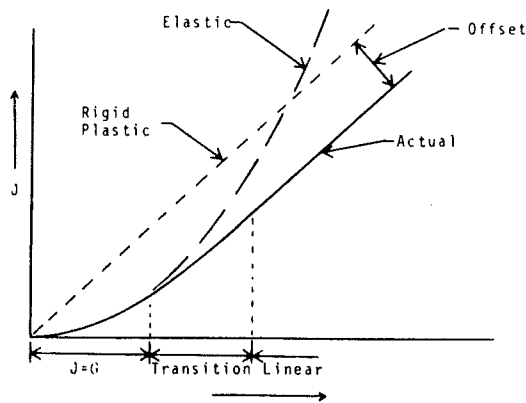
For the rigid plastic load-displacement relationship, deformation or  $\delta$  extension is unlimited at the limit load,  $P = P_L$ , while for  $P < P_L$ ,  $\delta = 0$ , Fig. 3a. Interpreting Eq 3 for  $J$  in terms of the area between two successive load displacement records,  $J$  as a function of  $\delta$  for the rigid plastic material is given as

$$J = -\frac{\delta}{B} \frac{\partial P_L}{\partial a} \quad (7)$$

where the derivative  $\partial P_L / \partial a$  is evaluated for the crack length of interest. The resulting rigid plastic expression for  $J$  is simply a linear function of  $\delta$ , and thus



(a) Typical Load Displacement (P vs.  $\delta$ ) Records



(b) Typical J vs.  $\delta$  Curves ( $a = \text{Constant}$ )

FIG. 3—Idealized versus actual behavior for load versus displacement and J versus displacement.

the  $J$  versus  $\delta$  relationship for constant crack size is a straight line emanating from the origin, Fig. 3b.

In reality actual load versus displacement characteristics border the two extremes exhibited by purely elastic and rigid plastic behavior, Fig. 3a. For low loads and associated small scale plasticity, a load-displacement behavior can always be approximated by linear elastic analysis giving a slope (or compliance) which is a function of crack size, specimen geometry, and elastic material constants. As loading progresses, increased plasticity introduces nonlinearity, and if fracture has not yet ensued prior to the attainment of limit load, a marked

increase in deflection, which ultimately leads to separation will occur without any substantial increase in load, Fig. 3a.

For a flawed configuration which sustains large scale yielding prior to fracture, it seems logical to expect similarly that the  $J$  versus  $\delta$  relationship also resembles the two extremes at low and high  $\delta$  (or  $J$ ). For small  $\delta$ , and consequently small scale plasticity,  $J$  can be represented simply by the linear elastic solution,  $J = G$ , which is parabolic in  $\delta$  for constant crack length. For large  $\delta$  where limit load is attained prior to fracture,  $J$  as a function of  $\delta$  becomes a linear relationship with a slope parallel to the idealized rigid plastic relationship, Fig. 3b. The offset between parallel segments of the rigid plastic and actual  $J$  versus  $\delta$  curves of Fig. 3b is governed in part by the nonlinearities in the  $P$  versus  $\delta$  records which occur in the transition region. Hence, estimation of the actual  $J$  versus  $\delta$  relationship rests on the ability to effectively approximate the elastic to plastic transition, or more specifically, the variation with crack length of the curved portion of the load displacement relationship up to limit load, as well as the limit load itself.

#### Estimation Techniques

A logical first attempt at providing estimated load-displacement records for successive crack sizes and hence,  $J$  versus  $\delta$  approximations would be to consider a family of purely elastic and perfectly plastic load-displacement records. For each particular crack size development of perfectly plastic behavior from the original elastic slope would occur at limit load, ignoring the nonlinear portion of the load-displacement relationships. Further, for fractures commencing after large deformations at limit load even the elastic portion might be ignored, proceeding in a manner consistent with Eq 7. However, it becomes evident that these first approximations are not adequate except for special situations and a more general approximation procedure would be advantageous.

A slightly more refined approximation can be made by amending the linear elastic portion of the load-displacement relationship analysis by use of an  $r_y$  plasticity adjustment factor [14] which considers the leading edge of the crack to be given a central location within the plastic zone [15]. The plasticity adjustment results in an equivalent elastic or effective crack size,  $a_{\text{eff}}$ , given by

$$a_{\text{eff}} = a + r_y \quad (8)$$

where

$$r_y = \frac{1}{2\pi} \left( \frac{K}{\sigma_{ys}} \right)^2 \quad (8a)$$

for plane stress and

$$r_y = \frac{1}{6\pi} \left( \frac{K}{\sigma_{ys}} \right)^2 \quad (8b)$$

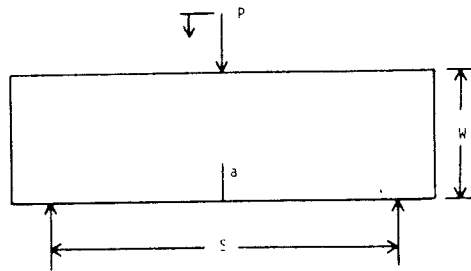


for plane strain.  $a$  is the actual crack size,  $K$  the stress intensity factor (based on actual crack size), and  $\sigma_{ys}$  the yield point (or small strain plastic flow stress) for the material in simple uniaxial tension. Utilization of the  $r_y$  plasticity adjustment appropriately introduces nonlinearity which is thought to be rather accurate for small scale yielding and which is at least more realistic than pure linear elastic analysis as yielding progresses. Employing the plasticity adjustment, a family of load-displacement records can be provided by using the plastically ( $r_y$ ) adjusted elastic analysis up to limit load and limit load analysis thereupon. A simple procedure used to apply the  $r_y$  plasticity adjustment to linear elastic load-displacement relations is discussed in Appendix 2.

Estimating schemes based on the observations cited above were tried and compared to existing Westinghouse experimental data on Ni-Cr-Mo-V (200-250 F) and A533 B(75 F) steels [1]. The three specimen configurations considered were the center notch, the three point bend bar (single and double thickness) for Ni-Cr-Mo-V steel, and the compact tension ( $H/W = 0.6$ ) for A533 B steel. The test configurations are sketched in Figs. 4 through 6.

#### *J* versus $\delta$ Computation and Analyses

Families of load displacement records developed by analytical estimation and by Westinghouse experiments, [1, 2], were curve fit by computer using an orthogonal polynomial relationship. The computational process was carried out in the manner prescribed in Appendix 1. That is, load displacement records were used to obtain apparent or "pseudo-potential energy" for constant displacement as a function of crack length (that is,  $U/B$  versus  $a$  curves). The  $U/B$  versus  $a$



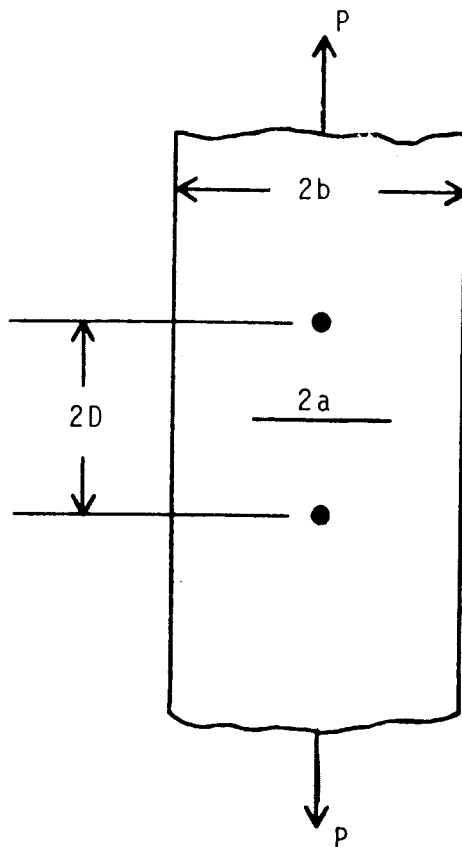
$B$  = Thickness = 0.394" and 0.788"

$W$  = 0.474"

$S$  = 1.57"

$\delta$  = Load Point Displacement

FIG. 4 - Westinghouse Ni-Cr-Mo-V three point bend bar test configuration.



$B = \text{Thickness} = 1.00''$

$2b = 1.00''$

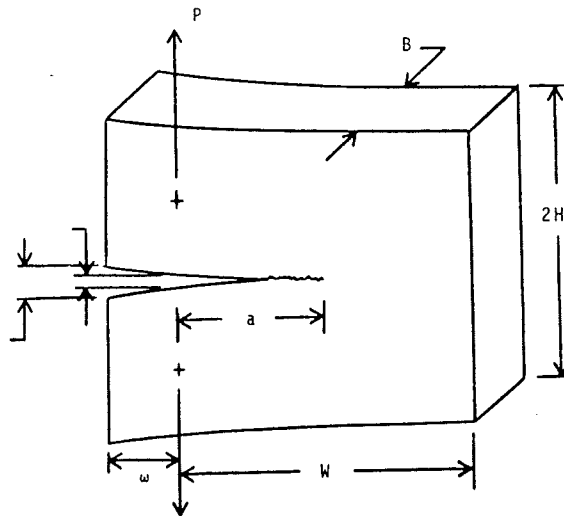
$2D = \text{Gage Length} = 2.25''$

FIG. 5—Westinghouse Ni-Cr-Mo-V center notch specimen configuration.

curves were best fit by a low order orthogonal polynomial and their slopes evaluated to yield  $J$  as a function of displacement,  $\delta$ , and crack size, consistent with Eq 3.<sup>5</sup>

Analytically estimated  $J$  versus  $\delta$  relationships for Ni-Cr-Mo-V steel specimens were compared to those obtained using actual Westinghouse load-displacement

<sup>5</sup>Since for the center notch specimen, the area between load-displacement records of neighboring crack sizes is representative of the total change in "pseudo-potential energy" for two cracks, an appropriate adjustment by a factor of 1/2 was necessary to evaluate  $J$  for each crack tip.



- $B = 1.00''$   
 $W = 2.00''$   
 $H = 1.20''$   
 $\omega = \text{Location of Gage from Load Line} = 5/8''$   
 $\delta = \text{Displacement at Load Line}$   
 $\delta' = \text{Displacement at Gage Location}$

FIG. 6—Westinghouse A533B compact tension test specimen configuration.

records [1]. For the A533 subsized compact tension test configuration, analytical estimates of the  $J$  versus  $\delta$  relationship were compared to the critical plane strain  $J$  ( $J_{Ic}$ ) and fracture displacement previously established by Westinghouse experiment on identical test configurations.

#### Development of Load Displacement Records for Each Specimen Configuration

##### Pure Elastic

Load-displacement relationships for the three point bend bar and center notch test configurations of Figs. 4 and 5 were analytically developed for pure elastic loading and are given below for the three point bend bar of Fig. 4 where  $\delta$  is measured at the point of load application.

$$\delta = \frac{0.24 PS^3}{BEW^3} [1.04 + 3.28 (W/S)^2 (1 + \nu)]$$

$$\begin{aligned}
& + \frac{2PS^2}{BE'W^2} \left(\frac{a}{W}\right) [4.21 \left(\frac{a}{W}\right) - 8.89 \left(\frac{a}{W}\right)^2 + 36.9 \left(\frac{a}{W}\right)^3 \\
& - 83.6 \left(\frac{a}{W}\right)^4 + 174.3 \left(\frac{a}{W}\right)^5 - 284.8 \left(\frac{a}{W}\right)^6 + 387.6 \left(\frac{a}{W}\right)^7 \\
& - 322.8 \left(\frac{a}{W}\right)^8 + 149.8 \left(\frac{a}{W}\right)^9]
\end{aligned} \tag{9}$$

where

$B, S, W, a$  are defined in Fig. 4, and  $E$  = Young's modulus,  
 $\nu$  = Poisson's ratio, and  
 $E' = E$  for plane stress  
 $= E/(1 - \nu^2)$  for plane strain.

For the center notch specimen of Fig. 5 where the gage is located a distance  $D$  above and below the center line of the crack

$$\begin{aligned}
\delta = \frac{P}{B} \left[ \frac{D}{bE} + \frac{4}{\pi E'} \left\{ \left(\frac{\pi a}{2b}\right)^2 \right. \right. \\
\left. \left. + \frac{1}{4} \left(\frac{\pi a}{2b}\right)^4 + \frac{5}{72} \left(\frac{\pi a}{2b}\right)^6 + \dots \right\} \right]
\end{aligned} \tag{10}$$

where  $B, D, b, a$  are defined in Fig. 5 and where  $E$  and  $E'$  have the same interpretation as above, and where it is assumed that  $D/a \gg 1$ . The derivation of Eqs 9 and 10 are outlined in Appendix 2.

Earlier established boundary collocation results [16, 17] were used to obtain load-displacement (at the load line and gage location) relationships for the compact tension specimen. A dimensionless plot of these results is given in Fig. 7.

For pure elastic loading, the  $J$  calculation could be simplified by acknowledging that  $J = G$ . Consequently, for a single crack tip,  $J$  can be calculated from

$$J = \frac{K^2}{E'} \tag{11}$$

where

$E' = E$  for plane stress  
 $= E/(1 - \nu^2)$  for plane strain

and  $K$  is simply the appropriate test configuration stress intensity factor.

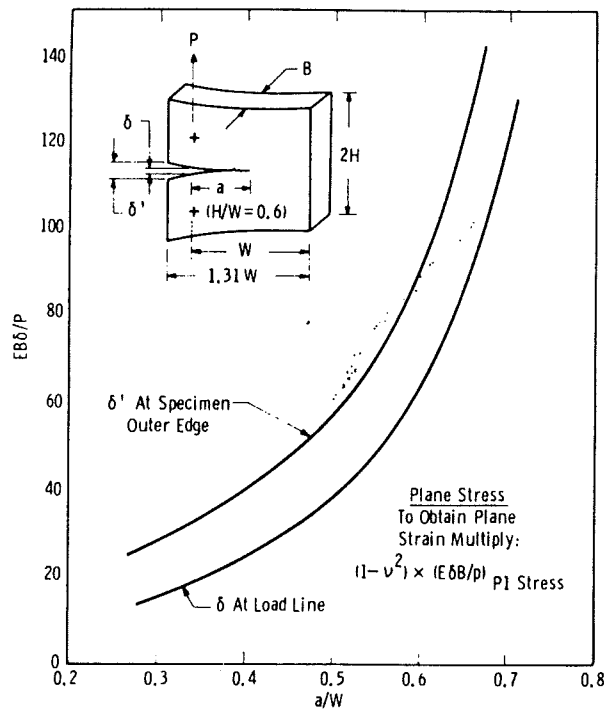


FIG. 7—Boundary collocation results for elastic loading of compact tension specimen [16, 17].

A tabulation of  $K$  calibrations used for the test configurations considered are given below for three point bend bar as shown in Fig. 4 [10]<sup>6</sup>

$$K = \frac{PS}{B(W)^{3/2}} \left[ 2.9 \left(\frac{a}{W}\right)^{1/2} - 4.6 \left(\frac{a}{W}\right)^{3/2} + 21.8 \left(\frac{a}{W}\right)^{5/2} - 37.6 \left(\frac{a}{W}\right)^{7/2} + 38.7 \left(\frac{a}{W}\right)^{9/2} \right] \quad (12)$$

For the center notch specimen, Fig. 5 [18]

$$K = \frac{P}{2Bb} \sqrt{\pi a \sec \frac{\pi a}{2b}} \quad (13)$$

<sup>6</sup>Equation 12 was obtained for a bend beam with  $S/W = 4$  [10, 20]. However, by extrapolation of results given in Ref 20, Eq 12 was found not to differ significantly from the expression obtained for a bend bar of  $S/W = 3.31$  (the actual  $S/W$  ratio for bend bar of Fig. 4).

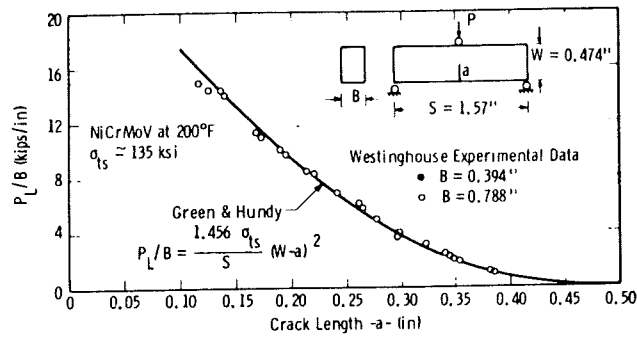


FIG. 8.—Limit load per unit thickness as a function of crack length for Westinghouse Ni-Cr-Mo-V three point bend test configuration.

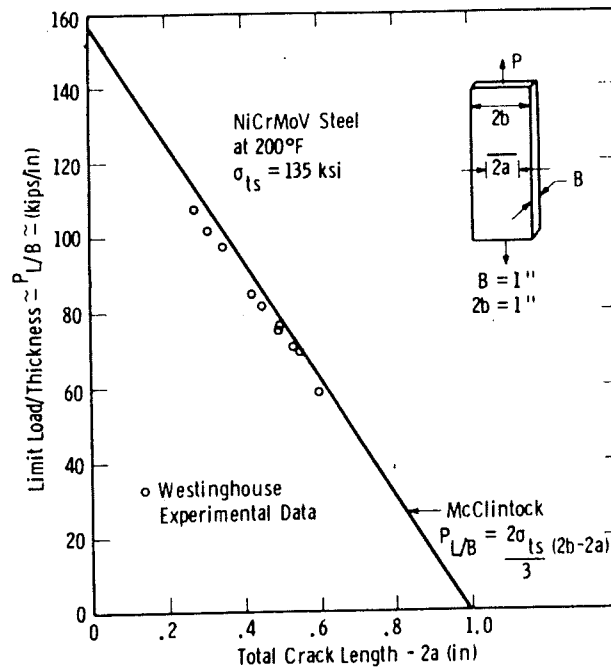


FIG. 9.—Limit load per unit thickness as a function of total crack length for Westinghouse Ni-Cr-Mo-V center notch test specimen configuration.

solution was found to be quite sufficient when compared to actual Westinghouse limit load data on A533 B steel ( $\sigma_{ys} \approx 70$  ksi) 1TCT and 2TCT compact tension specimens [1], Fig. 10.<sup>7</sup>

To compute the  $J$  versus  $\delta$  relationship for rigid plastic material behavior, one could use the procedure outlined in Appendix 1 or more simply employ Eq 7. Rewriting Eq 7 to consider the possibility of more than one crack tip:

$$J = - \frac{\delta}{B} \frac{\partial P_L}{\partial (\alpha a)} \tag{18}$$

where  $\alpha = 1$  for configurations with one crack tip  
 $\alpha = 2$  for configurations with two crack tips

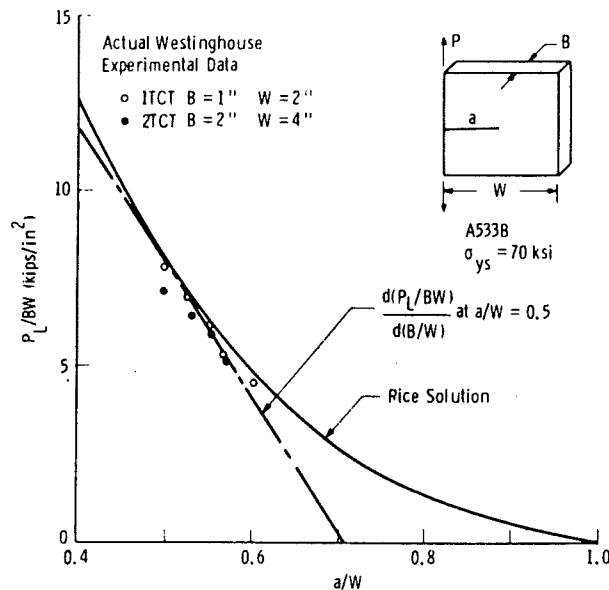


FIG. 10--Limit load divided by  $BW$  as a function of dimensionless crack size,  $a/W$  for Westinghouse A533B compact tension specimen.

<sup>7</sup>In order to calculate limit load for the three configurations, uniaxial tensile strength was employed in Eqs 16 and 17 for the bend bar and center notch configuration, whereas the Rice approximation for the compact tension configuration contains yield strength. The above selection was based upon success demonstrated by Eqs 16 and 17 and the Rice procedure in predicting actual limit load, refer to Figs. 8 through 10. For a mild steel alloy, subsequent unpublished results have shown when final fracture occurs prior to the attainment of full limit load conditions, the critical  $J$  estimation is rather insensitive to precise definition of a suitable plastic flow parameter for example,  $\sigma_{ys}$ ,  $\sigma_{TS}$ ,  $1/2 (\sigma_{ys} + \sigma_{TS})$ , etc.). For the mild steel investigated ( $\sigma_{ys \text{ min}} = 50$  ksi  $\sigma_{TS \text{ min}} = 80$  ksi) a  $\pm 10$  percent variation in averaged flow stress resulted in critical  $J$  estimates within  $\pm 15$  percent.

Thus for the bend bar

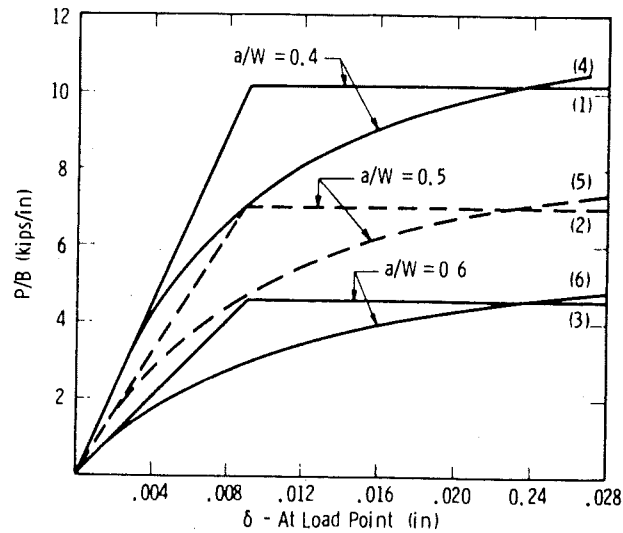
$$J = 2.912 \sigma_{ts} \frac{\delta}{S} (W - a) \quad (19)$$

and for the center notch specimen

$$J = \frac{2\sigma_{ts}}{\sqrt{3}} \delta \quad (20)$$

For the compact tension specimen  $\partial P_L / \partial a$  could be determined graphically, Fig. 10, and substituted into Eq 18.

For the three chosen specimen configurations, Figs. 11 through 13 show typical analytically generated load displacement records for three different crack sizes for both the elastic (plane stress), perfectly plastic, and the elastic (plane



NiCrMoV  
 Bend Bar (S = 1.57" W = 0.474")  
 B = 0.394" Single Size  
 B = 0.788" Double Size  
 E =  $30 \times 10^3$  ksi

(1), (2), (3) Elastic (plane stress) perfectly plastic  
 (4), (5), (6) Elastic (plane stress with plane stress plasticity adjustment)

FIG. 11—Typical estimated load displacement relationships for Westinghouse Ni-Cr-Mo-V single and double thickness three point bend bars.



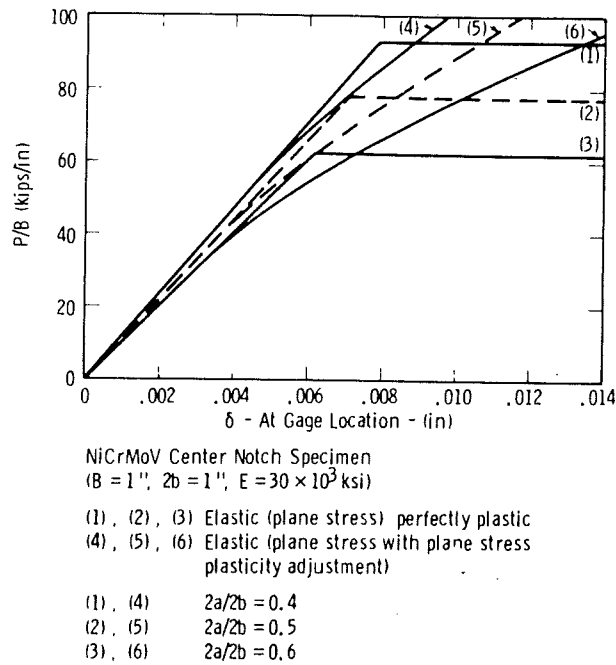


FIG. 12—Typical estimated load displacement relationships for Westinghouse Ni-Cr-Mo-V center notch specimen.

stress) with plane stress plasticity adjustment assumptions. An even better approximation of actual load-displacement records may be obtained by taking the plastically adjusted elastic behavior for loads less than limit load with a switch to perfectly plastic behavior at limit load.

Elastic load displacement relationships were chosen to be those for plane stress which differs from that of plane strain *at most* by a factor of  $(1 - \nu^2) \approx 0.90$ . (This can be verified upon examination of Fig. 7 and Eqs 9 and 10). Use of the plane stress plasticity adjustment, Eq 8a, is justified by having a specimen *thickness* which gives plane stress conditions for most of the plastic zone (during the time the correction is used). Even so, it is the difference between load-displacement curves for changes in crack length which seems best approximated here by plane stress. However, thicker specimens (all other dimensions remaining equal) might require use of a plane strain adjustment factor, for example, Eq 8b.

Figure 14 presents a typical comparison between plane stress and plane strain estimations of load displacement behavior for the A533 B compact tension specimen considered. The area beneath both pure elastic (plane stress and plane strain) and plane strain plastically adjusted curves are essentially similar. Thus, it appears that pragmatic selection of a plane stress plasticity adjustment is justified for the specimen configuration and size considered.

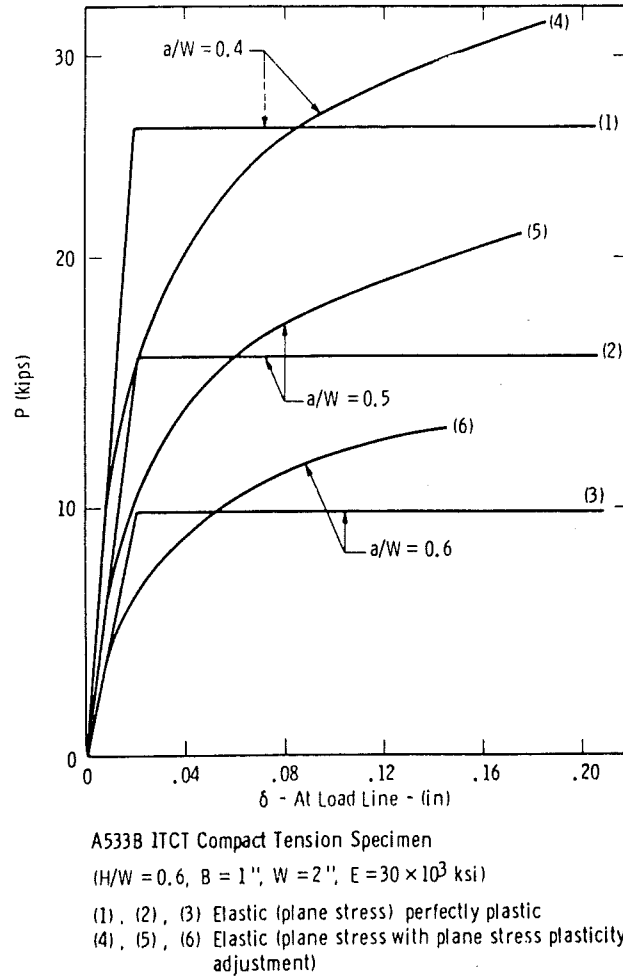


FIG. 13—Typical estimated load displacement relationships for Westinghouse A533B ITCT compact tension specimen.

It is perhaps worthy of note that the bend specimen and compact tension specimen estimated deflection at limit load (both for perfectly elastic and plastically adjusted loading) is rather insensitive to crack length for the range of  $a/W$  ratios plotted on Figs. 11 and 13. On the other hand, from Fig. 12, estimated center notch specimen limit load deflection appears to be somewhat sensitive to crack length. This sensitivity might suggest that the center notch configuration is more difficult to develop approximations for  $J$  integral calculation than either of the other two configurations.

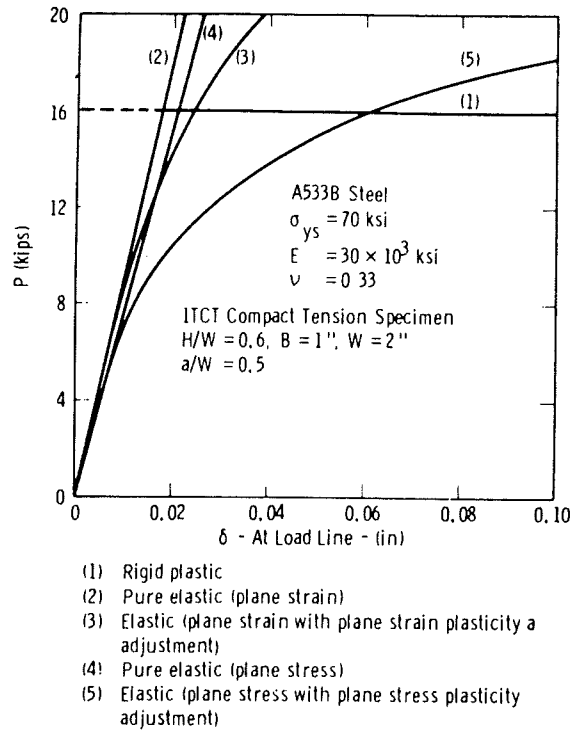


FIG. 14 Typical estimated load displacement relationships for Westinghouse A533B ITCT compact tension specimen,  $a/W = 0.5$ .

## Results

For the Ni-Cr-Mo-V single and double thickness, three point bend bars of geometry prescribed in Fig. 4, Fig. 15 presents  $J$  as a function of  $\delta$  determined from both analytically approximated and Westinghouse experimentally established load displacement records. Results for a crack length to width ratio,  $a/W$ , equal to 0.50 are shown; however,  $a/W$  ratios of 0.40 and 0.60 were also tried and found to give essentially similar comparisons. The analytical model does not involve thickness except for the "either-or" choice of plane stress or plane strain. Hence, for in-plane specimen geometry of Fig. 4, analytically estimated results (Fig. 15) were independent of thickness, while those results based on experiment exhibited a slight change with thickness. However, it should be noted that the specimen of smallest thickness ( $B = 0.394$  in.) did not quite meet a "degree of plane strain" requirement based on experimental observations of Begley and Landes [1, 9]. Based on their observations for the specimen geometry considered, an approximate thickness  $B = 0.42$  in. would be required to satisfy the "degree of plane strain" requirements. Greater than this thickness (namely,  $B > 0.42$  in.) experimental results should be essentially thickness insensitive.

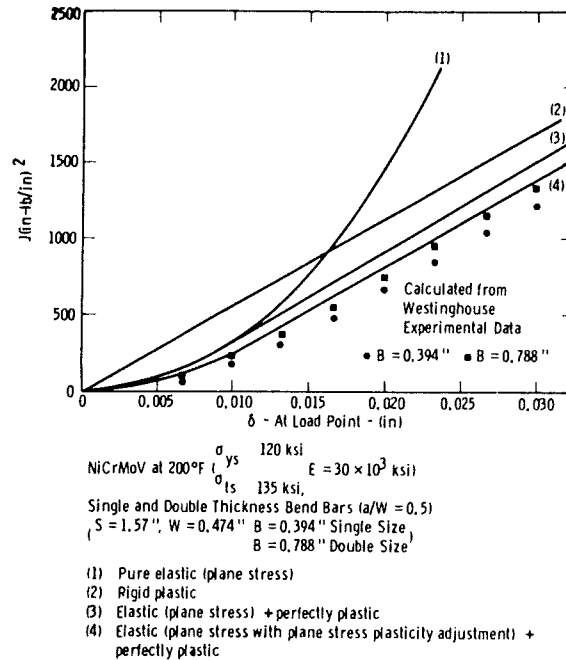


FIG. 15— $J$  as a function of load point displacement,  $\delta$ , for Westinghouse Ni-Cr-Mo-V single and double thickness bend bars.

Experimental results of the thicker specimen ( $B = 0.788$  in.) shown in Fig. 15 satisfy such a requirement.

Of the various analytical schemes tried, those results derived from load-displacement behavior considered to be elastic plane stress,  $r_y$  plasticity adjusted, plus perfectly plastic (curve 4) agreed best with those results computed from the Westinghouse experimental data. Analytical agreement with experimental data was best for the thick specimen.

For both the single and double thickness bend bars, Westinghouse experimentally determined displacement,  $\delta$ , at fracture ranged between 0.22 and 0.24 in. for  $a/W$  ratios of magnitude comparable to 0.5. Employing these experimentally determined fracture displacements and the  $a/W = 0.5$   $J$  versus  $\delta$  relationship approximated by plastically adjusted elastic plane stress plus perfectly plastic loading (curve 4, Fig. 15), an estimated range of critical  $J$  would be 900-1100 in.·lb/in.<sup>2</sup> This agrees very well with an average critical plane strain  $J(J_{IC})$  of 1000 in.·lb/in.<sup>2</sup> experimentally established by Begley and Landes [1] and is also within good agreement<sup>8</sup> with upper shelf

<sup>8</sup>Since  $J_{IC}$  is determined for the beginning of crack extension and  $G_{IC}$  for a 2 percent crack extension, it follows that  $G_{IC}$  should be larger than  $J_{IC}$ .

(200 F)  $G_{Ic} = 1200 \text{ in.} \cdot \text{lb/in.}^2$  established from Westinghouse  $K_{Ic}$  fracture toughness tests on thicker test specimens [1, 24].

For the Ni-Cr-Mo-V center notch specimen, a comparison of  $J$  versus  $\delta$  relationships based upon analytical and experimental load displacement records are presented, Fig. 16, for,  $2a/2b = 0.5$ . Crack length to width ratios  $2a/2b = 0.4$  and  $0.6$  were also tried and found to yield similar comparisons. Again,  $J$  versus  $\delta$  agreement of actual experiment and assumed elastic-plastic adjusted (plane stress) perfectly plastic loading (curve 4) are quite good. For comparable crack lengths, a Westinghouse experimentally determined  $\delta$  at fracture was generally found to be in the range of 0.016 and 0.018 in. which corresponds to an estimated central  $J$  range, 800-900  $\text{in.} \cdot \text{lb/in.}^2$ . This is in excellent agreement with previous Ni-Cr-Mo-V results and is well within the experimental bounds of fracture toughness determination of rotor steels for which  $K_{Ic}$  may vary as much as 15 percent, and which corresponds to a  $J$  critical variation of as much as  $\pm 30$  percent [1].

Analytical  $J$  versus  $\delta$  estimations for an A533 compact tension (CT) specimen,  $a/W = 0.5$ , are presented in Fig. 17. For the 1-in.-thick CT specimen,  $W$  equaled 2.00 in., and gage location was at the specimen outer edge,  $5/8$  in. from the load line (corresponding to a total specimen width of  $1.31 W$ ). For the 1-in. CT specimen,  $a/W = 0.5$ , gage location deflection at fracture was

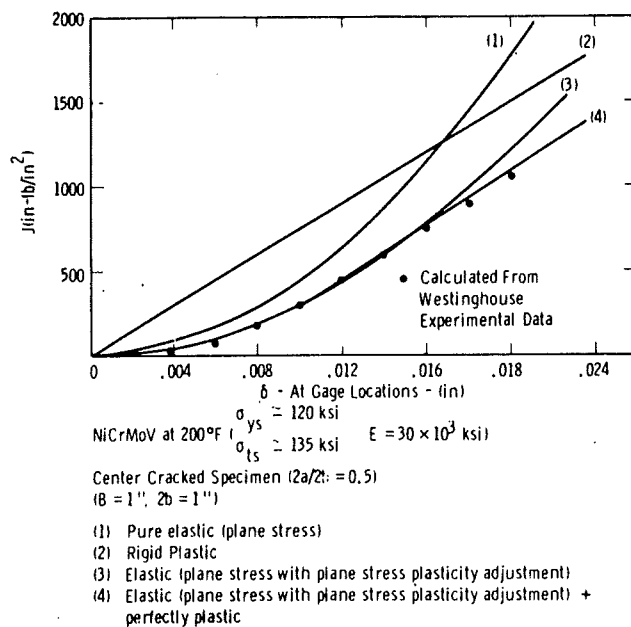


FIG. 16— $J$  as a function of gage point displacement,  $\delta$ , for Westinghouse Ni-Cr-Mo-V center notch test specimen.

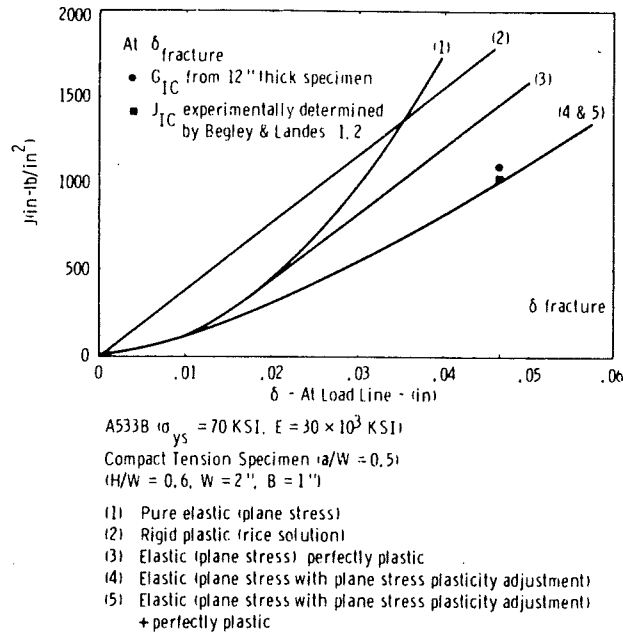


FIG.17 -  $J$  as a function of load line displacement,  $\delta$ , for Westinghouse A533B compact tension test specimen.

experimentally determined to be 0.07 in. [1]. Boundary collocation results on the CT specimen in Fig. 7 indicate that  $a/W = 0.5$  load line deflection is approximately two-thirds of that deflection at the outer specimen edge. This implies that a gage deflection of 0.07 in. corresponds to a load line deflection of 0.0467 in. For a load line fracture deflection of 0.0467 in. a critical value of  $J$  estimated for elastic (plastically adjusted) plus perfectly plastic loading is found to be 1025 in. $\cdot$ lb/in.<sup>2</sup>, Fig. 17. This is in extraordinary agreement with the Westinghouse experimentally determined plane strain critical  $J$  value ( $J_{1C} = 1030$  in. $\cdot$ lb/in.<sup>2</sup>) for the same material test configuration [1]. The estimated critical  $J$  is also in very good agreement with plane strain ( $G_{1C} = 1100$  in. $\cdot$ lb/in.<sup>2</sup>) results converted from fracture toughness measurements on specimens 12 inches thick [1].

Consequently, upon examination of Figs. 15 through 17, it appears that very simple estimation of elastic perfectly plastic  $J$  versus  $\delta$  may be provided from extension of a line parallel to the rigid plastic solution at its point of tangency with the plasticity adjusted elastic solution.

### Summary

For the materials and test configurations considered, reasonable estimations of the  $J$  versus  $\delta$  relationship were made utilizing generated load displacement

records assumed to be plane stress, plastically adjusted linear elastic, plus perfectly plastic.

Provided that suitable approximations of the  $J$  versus  $\delta$  relationship exist, it appears that critical  $J$  estimations, for a particular material test configuration, could be obtained given the additional experimental knowledge of the load point deflection  $\delta$  at the inception of fracture. For a given flaw size, a minimum of one (or possibly two) experimental load displacement record(s) would be sufficient to establish this information, along with the analytical procedures demonstrated herein.

Employing these procedures, and utilizing Westinghouse data [1], analytical predictions of critical plane strain  $J$  ( $J_{Ic}$ ) were found to agree quite well with Westinghouse  $J_{Ic}$  results [1]. Moreover, the estimated critical  $J$  was also found to agree quite well with  $G_{Ic}$  as determined from state-of-the-art valid plane strain ( $K_{Ic}$ ) fracture toughness tests.

It also becomes apparent that the ability to effect reasonable approximations of the  $J$  versus  $\delta$  relationship does not rest entirely on an ability to estimate load displacement behavior with great precision. Instead,  $J$  versus  $\delta$  approximation appears to be appropriately related to estimating characteristic changes in load displacement behavior with changing flaw size.

The  $J$  versus  $\delta$  estimation technique considered herein, which utilizes no more than elements of linear elastic fracture mechanics and plastic limit analysis, appears to offer considerable promise in application related to elastic-plastic failure analysis of complex engineering structures for which it might be difficult to obtain exact solutions for the relationship.

#### *Acknowledgments*

We fully acknowledge sponsorship of this work by Westinghouse Research Laboratories' Fracture Mechanics Group. Special acknowledgment is due to E.T. Wessel, manager of the Westinghouse Fracture Mechanics Group, for his leadership, cooperation, and interest which helped greatly to stimulate the progress of this work, and, similarly, acknowledgment is due to his co-worker, J.A. Begley with whom we worked very closely.

We are extremely grateful to S. Shadle and R. Lane of Del Research for their development of suitable computer programs and for their effective assistance through all the numerical work. In addition, acknowledgment is made to J.A. McCall for her secretarial assistance.

## APPENDIX 1

### Computation of $J$ as a Function of $\delta$ from a Family of Load-Displacement Records [1]

Given a typical test specimen configuration, Fig. 18a, load-displacement ( $P$ - $\delta$ ) records are obtained for a number of constant crack lengths, Fig. 18b. For given

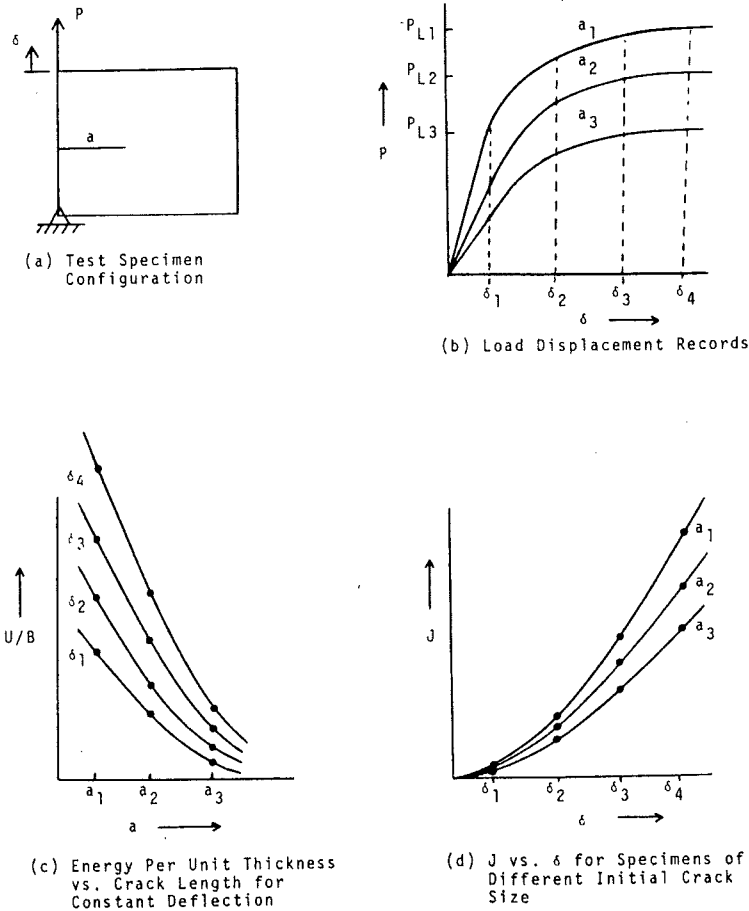


FIG. 18—Schematic diagram of  $J$  versus  $\delta$  evaluation employing a family of load displacement records.

values of deflection,  $\delta$ , the area under each load-displacement record may be interpreted as "pseudo-potential energy" of the body at that displacement. This can then be plotted, Fig. 18c, as pseudo-potential energy normalized per unit thickness,  $U/B$ , versus crack length,  $a$ , for constant  $\delta$ . Following Eq 3,  $J$  may be interpreted as the area between load-displacement curves of neighboring crack size, or more simply as the negative slope of the  $U/B$  versus  $a$  curves, for given constant  $\delta$ . This permits evaluation of a  $J$  versus  $\delta$  relationship which is also a function of crack size, Fig. 18d. Given the  $J$  versus  $\delta$  relationship for a given crack size, an experimentally determined fracture displacement which characterizes onset of unstable fracture may be used to determine a critical  $J$ .



## APPENDIX 2

## Calculation of Elastic and Plastically Adjusted Load-Displacement Relationships

*Three Point Bend Bar*

For the three point bend bar of Fig. 4 where  $\delta$  is the deflection of the load point, an elastic compliance calibration may be derived as follows [14].

Define  $U_{\text{tot}}$  as the total amount of strain energy stored in a cracked bend bar. The total strain energy may be divided into that which would exist if no crack were present, plus that which is due to the introduction of a crack. That is,

$$U_{\text{tot}} = U_{\text{no crack}} + U_{\text{due to crack}} \quad (21)$$

The no crack contribution may simply be divided into bending and shear contributions which can be calculated from well known strength of material results [25]. That is,

$$U_{\text{no crack}} = U_{\text{bending}} + U_{\text{shear}}$$

where

$$U_{\text{bending}} = \int_0^s \frac{M^2 dx}{2EI}$$

$$M = 1/2 Px$$

and

$$U_{\text{shear}} = \int_{-w/2}^{w/2} \int_0^s \frac{\tau^2}{2G} B dx dy$$

where

$$\tau = \frac{V}{IB} \int_y^{w/2} y dA$$

$I$  = moment of inertia,  $E$  = elastic modulus,  $G$  = shear modulus,  $\tau$  = shear stress,  $M$  = cross sectional bending moment,  $V$  is average shear force across a cross sectional area, all other symbols are defined in Fig. 4.

To determine the strain energy contribution due to the crack, one may recall from the Griffith approach [7, 8, 13, 26] that  $G$ , the energy available for crack extension, is defined as

$$G = \frac{\partial U_{\text{due to crack}}}{B \partial a} \quad (22)$$

from which

$$U_{\text{due to crack}} = B \int_0^a G da$$

Converting  $G$  to  $K$ , the stress intensity factor

$$U_{\text{due to crack}} = \frac{B}{E'} \int_0^a K^2 da$$

where

$$\begin{aligned} E' &= E \text{ for plane stress} \\ &= E/(1 - \nu^2) \text{ for plane strain} \end{aligned}$$

and

$$K = \frac{PS}{BW^{3/2}} F\left(\frac{a}{W}\right)$$

is the form of the stress intensity expression for the three point bend bar, Eq 12. The total deflection  $\delta_{\text{tot}}$  may be summed as a contribution without the crack plus a contribution due to the crack. That is,

$$\delta_{\text{tot}} = \delta_{\text{no crack}} + \delta_{\text{due to crack}} \quad (23)$$

Employing Castigliano's theorem and Eqs 21-23

$$\delta_{\text{tot}} = \frac{\partial U_{\text{tot}}}{\partial P} = \frac{\partial U_{\text{no crack}}}{\partial P} + \frac{\partial U_{\text{due to crack}}}{\partial P}$$

which gives  $\delta$  as a linear function  $P$

$$\delta = P \times F'(a/W, S, B, W, E, \nu)$$

For the configuration of Fig. 4, this relationship is given by Eq 9.

#### *Center Notch Specimen*

For the center notch specimen of Fig. 5, one may compute the compliance relationship as follows. Two components of deflection may be considered as that due to the crack and that which would exist if no crack were present. From which,

$$\delta_{\text{tot}} = \delta_{\text{no crack}} + \delta_{\text{due to crack}} \quad (24)$$

$\delta_{\text{no crack}}$  is simply,

$$\delta_{\text{no crack}} = \frac{P(2D)}{(2bB)E} \quad (25)$$

where all specimen dimensional symbols are given in Fig. 5. To find the contribution of the crack, the total energy release rate for the two crack tips may be written as

$$G = \frac{P^2 \partial \lambda}{2(2B \partial a)}$$

but  $G = K^2/E' + K^2/E'$  (since there are two cracks) and,

$$\lambda = \frac{\delta_{\text{due to crack}}}{P} = \frac{4B}{P^2 E'} \int_0^a K^2 da \quad (26)$$

employing the appropriate stress intensity factor, Eq 13, a  $\delta$  contribution due to the crack may be computed. Summing the deflection contributions given by Eqs 25 and 26 results in a final compliance relationship given by Eq 10 where higher order terms are neglected.

#### *r<sub>y</sub> Plasticity Adjustment*

A simple technique for applying an  $r_y$  plasticity adjustment to a linear elastic load displacement relationship can be illustrated as follows.

Consider that by linear elastic fracture mechanics techniques a purely elastic compliance relationship has been developed. A typical relationship for a compact tension specimen is graphically represented in Fig. 19a where compliance is dimensionlessly plotted as a function of dimensionless crack size. Employing the plasticity adjustment suggested by Eqs 8 and 8a

$$\frac{a_{\text{eff}}}{W} = \frac{1}{W} \left[ a_0 + r_y \right] = \frac{1}{W} \left[ a_0 + \frac{1}{2\pi} \left( \frac{K}{\sigma_{ys}} \right)^2 \right] \quad (27)$$

where  $a_0$ , is the actual original crack size. Typically, substituting the stress intensity expression for a compact tension specimen, Eq 27 becomes

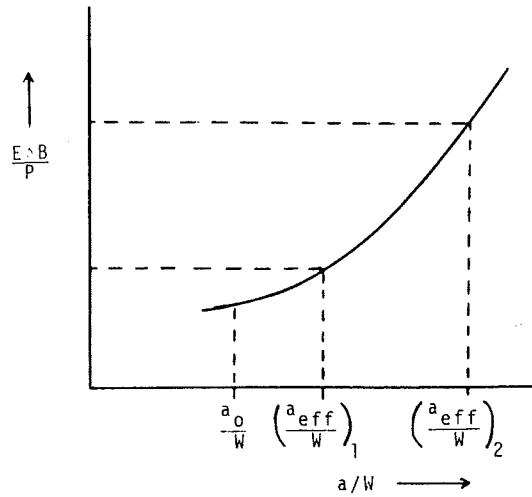
$$\frac{a_{\text{eff}}}{W} = \frac{a_0}{W} + \frac{P^2 F^2 \left( \frac{a_0}{W} \right)}{2\pi B^2 W^2 \sigma_{ys}^2} \quad (28)$$

for a given load  $P_1$ , an  $\left( \frac{a_{\text{eff}}}{W} \right)_1$  may be computed from Eq 28 as

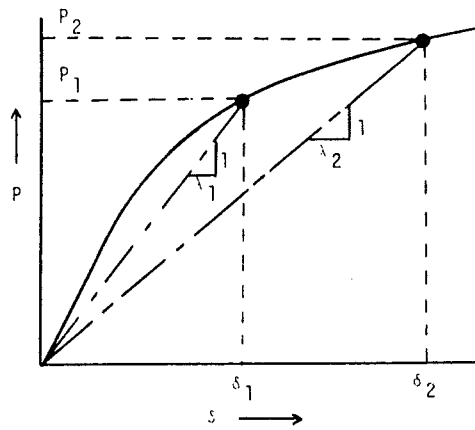
$$\left( \frac{a_{\text{eff}}}{W} \right)_1 = \frac{a_0}{W} + \frac{P_1^2 F^2 \left( \frac{a_0}{W} \right)}{2\pi B^2 W^2 \sigma_{ys}^2}$$

from which an adjusted  $(E\delta B/P)_1$  may be determined from Fig. 19a. Having  $P_1$  and  $(E\delta B/P)_1$  known, as adjusted deflection,  $\delta_1$ , can be computed as

$$\delta_1 = \left( \frac{E \delta B}{P} \right)_1 \frac{P_1}{Eb}$$



(a) Typical Compliance Relationship



(b) Load vs. Displacement

FIG. 19--Sample calculation of  $\lambda_y$  plasticity adjusted load displacement records.

Hence,  $P_1$  and  $\delta_1$  are known and can be plotted as a point on a load displacement record, Fig. 19b. The same procedure may be followed to generate a series of points  $(P_2, \delta_2) \dots (P_n, \delta_n)$  which will produce a plastically adjusted elastic load displacement record for a given initial crack size.

## References

- [1] Begley, J.A. and Landes, J.D., "The  $J$  Integral as a Fracture Criterion," and "The Effect of Specimen Geometry on  $J_{IC}$ ," *Fracture Toughness, Proceedings of the 1971 National Symposium on Fracture Mechanics, ASTM STP 514*, American Society for Testing and Materials, 1972, pp. 1-20 and 24-39.
- [2] Rice, J.R., *Journal of Applied Mechanics, Transactions of the American Society of Mechanical Engineers*, June 1968, pp. 379-386.
- [3] Hayes, D.J., "Some Applications of Elastic-Plastic Analysis of Fracture Mechanics," Ph.D. dissertation, Department of Mechanical Engineering, Imperial College, University of London, Oct. 1970.
- [4] W.K. Wilson and S.K. Chan, private communication, Westinghouse Research Laboratories, Pittsburgh, Pa., 1971.
- [5] Levy, N., Ostergren, W.J., Marcal, P.V., and Rice, J.R., *International Journal of Fracture Mechanics*, Vol. 7, No. 2, 1971, pp. 143-156.
- [6] Rice, J.R. in *Fracture*, Vol. II, Academic Press, New York, 1968.
- [7] Irwin, G.R., *Welding Journal Research Supplement*, 1954.
- [8] Irwin, G.R., *Journal of Applied Mechanics, Transactions of the American Society of Mechanical Engineers*, 1957.
- [9] Paris, P.C., Discussion in *Fracture Toughness, Proceedings of the 1971 National Symposium on Fracture Mechanics, ASTM STP 514*, American Society for Testing and Materials, 1972, pp. 21-23.
- [10] Irwin, G.R., "Plasticity Characterizations of Progressive Crack Extension," comments made at ASTM E 24 Task Group meeting, ASTM Headquarters, Philadelphia, 8 Sept. 1971.
- [11] "Tentative Method of Test for Plane Strain Fracture Toughness of Metallic Materials," ASTM E 399-70T; also, *Review of Developments in Plane Strain Fracture Toughness Testing, ASTM STP 463*, American Society for Testing and Materials, 1970.
- [12] McClintock, F.A., in *Fracture*, Vol. III, Academic Press, New York, 1971.
- [13] Paris, P.C. and Sih, G.C. in *Fracture Toughness Testing and Its Applications, ASTM STP 381*, American Society for Testing and Materials, 1965.
- [14] Paris, P.C., "The Mechanics of Fracture Propagation and Solutions to Fracture Arrestor Problems," Document D2-2195, Boeing Company, 1957.
- [15] Irwin, G.R. and Paris, P.C. in *Fracture*, Vol. III, Academic Press, New York, 1971.
- [16] Gross, B., Roberts, E., and Srawley, J.E., *International Journal of Fracture Mechanics*, Vol. 4, No. 3, Sept. 1968.
- [17] Roberts, E., *Materials Research and Standards, MTRSA*, Vol. 9, No. 2, Feb. 1969.
- [18] Feddersen, C., Discussion to *Plane Strain Crack Toughness Testing of High Strength Metallic Materials, ASTM STP 410*, American Society for Testing and Materials, 1967, p. 77.
- [19] Wessel, E.T., *Journal of Engineering Fracture Mechanics*, Vol. 1, No. 1, 1968, p. 77f.
- [20] Brown, W.F., Jr., and Srawley, J.E., *Plane Strain Crack Toughness Testing of High Strength Metallic Materials, ASTM STP 410*, American Society for Testing and Materials, 1966, p. 13.
- [21] Green, A.P. and Hundy, B.B., *Journal of the Mechanics and Physics of Solids*, Vol. 4, 1956, pp. 128-144.
- [22] McClintock, F.A., *Welding Journal Research Supplement*, Vol. 26, 1961, pp. 202-208.
- [23] Rice, J.R., "The Line Spring Model for Surface Flaws" to be published in Proceedings of the Surface Flaw Symposium, ASME Winter Annual Meeting, Nov. 1972.
- [24] Begley, J.A. and Toolin, P.R., "Fracture Toughness and Fatigue Crack Growth Rate Properties of a Ni-Cr-Mo-V Steel Sensitive to Temper Embrittlement," presented at the Fourth National Symposium on Fracture Mechanics, Carnegie-Mellon University, Pittsburgh, Pa., Aug. 1970.
- [25] Den Hartog, J.P., *Strength of Materials*, McGraw Hill, New York, 1949.
- [26] Griffith, A.A., *Philosophical Transactions of the Royal Society*, Vol. A-221, 1920.